(12) INTERNATIONAL APPLICATION PUBLISHED UNDER THE PATENT COOPERATION TREATY (PCT)

(19) World Intellectual Property Organization
International Bureau

(43) International Publication Date
27 May 2010 (27.05.2010)

PCT

(10) International Publication Number
WO 2010/059476 A1

(51) International Patent Classification:
A61F 2/46 (2006.01) *G01M 5/00* (2006.01)

(21) International Application Number:
PCT/US2009/064019

(22) International Filing Date:
11 November 2009 (11.11.2009)

(25) Filing Language: English

(26) Publication Language: English

(30) Priority Data:
12/273,844 19 November 2008 (19.11.2008) US

(71) Applicant *(for all designated States except US)*: **BOARD OF TRUSTEES OF MICHIGAN STATE UNIVERSITY** [US/US]; 246 Administration Building, East Lansing, Michigan 48824-1046 (US).

(72) Inventor; and

(75) Inventor/Applicant *(for US only)*: **CHAKRABARTTY, Shantanu** [IN/US]; Michigan State University, C/o 246 Administration Building, East Lansing, Michigan 48824 (US).

(74) Agents: **FALCOFF, Monte, L.** et al.; Harness, Dickey & Pierce, P.L.C., P.O. Box 828, Bloomfield Hills, Michigan 48303 (US).

(81) Designated States *(unless otherwise indicated, for every kind of national protection available)*: AE, AG, AL, AM, AO, AT, AU, AZ, BA, BB, BG, BH, BR, BW, BY, BZ, CA, CH, CL, CN, CO, CR, CU, CZ, DE, DK, DM, DO, DZ, EC, EE, EG, ES, FI, GB, GD, GE, GH, GM, GT, HN, HR, HU, ID, IL, IN, IS, JP, KE, KG, KM, KN, KP, KR, KZ, LA, LC, LK, LR, LS, LT, LU, LY, MA, MD, ME, MG, MK, MN, MW, MX, MY, MZ, NA, NG, NI, NO, NZ, OM, PE, PG, PH, PL, PT, RO, RS, RU, SC, SD, SE, SG, SK, SL, SM, ST, SV, SY, TJ, TM, TN, TR, TT, TZ, UA, UG, US, UZ, VC, VN, ZA, ZM, ZW.

(84) Designated States *(unless otherwise indicated, for every kind of regional protection available)*: ARIPO (BW, GH, GM, KE, LS, MW, MZ, NA, SD, SL, SZ, TZ, UG, ZM, ZW), Eurasian (AM, AZ, BY, KG, KZ, MD, RU, TJ, TM), European (AT, BE, BG, CH, CY, CZ, DE, DK, EE, ES, FI, FR, GB, GR, HR, HU, IE, IS, IT, LT, LU, LV, MC, MK, MT, NL, NO, PL, PT, RO, SE, SI, SK, SM, TR), OAPI (BF, BJ, CF, CG, CI, CM, GA, GN, GQ, GW, ML, MR, NE, SN, TD, TG).

Declarations under Rule 4.17:

— *as to applicant's entitlement to apply for and be granted a patent (Rule 4.17(ii))*

— *as to the applicant's entitlement to claim the priority of the earlier application (Rule 4.17(iii))*

Published:

— *with international search report (Art. 21(3))*

(54) Title: SELF-POWERED SENSOR

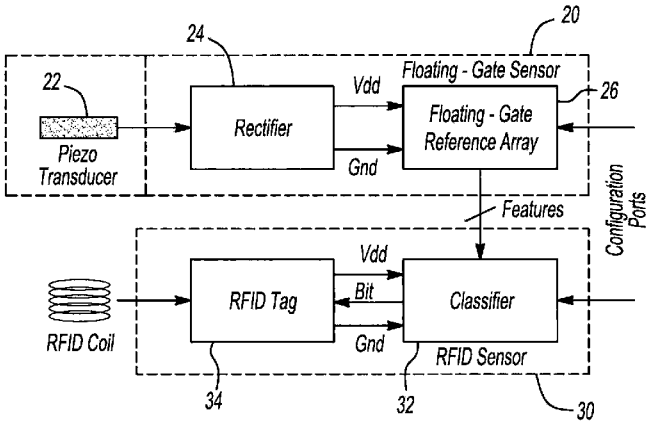


Fig-2

(57) Abstract: A self-powered sensor (20) is provided for strain-rate monitoring and other low power requirement applications. The self -powered sensor is comprised of : a piezoelectric transducer (22); a non-volatile memory comprised of at least one floating gate transistor; a current reference circuit adapted to receive a voltage signal from the piezoelectric transducer and operable to output a reference current into the non-volatile memory; an impact-monitoring circuit having a triggering circuit and a switch; the triggering circuit adapted to receive the voltage signal from the piezoelectric transducer and operable to control the switch based on the rate of change of the voltage signal.

WO 2010/059476 A1

SELF-POWERED SENSOR

CROSS-REFERENCE TO RELATED APPLICATIONS

[0001] This application claims priority to United States Patent Application No. 12/273,844 filed November 19, 2008, which is a continuation-in-part of United States Patent Application Serial Number 11/895,635 filed August 24, 2007, which claims the benefit of United States Provisional No. 60/840,056, filed August 24, 2006, which are all incorporated by reference herein.

GOVERNMENT RIGHTS

[0002] The U.S. Government may have a paid-up license in this invention, and may have the right, in limited circumstances, to require the patent owner to license others on reasonable terms as identified by the terms of Federal Grant No. CMMI-0700632 awarded by the NSF.

FIELD

[0003] The present disclosure relates to a self-powered sensor.

BACKGROUND

[0004] Approximately 500,000 hip and knee replacements are performed each year in the United States. Although these implants exhibit excellent response during the initial rehabilitation period, fatigue and wear limits their success for long-term operation. Monitoring of fatigue and wear has been previously shown to increase implant longevity by preventing mechanical failure through early intervention. Mechanical fatigue is the accumulation of damage in a structure under applied fluctuating stresses. Though the magnitudes of the applied stresses are less than the tensile strength of the material, the progressive fatigue damage may lead ultimately to mechanical failure. Fatigue life is defined as the number of load cycles necessary to induce failure and it depends on the level of fluctuating strain in the structure. Several fatigue prediction algorithms (e.g. Palmgren-Miner linear rule) rely on counting the number and magnitude of loading cycles applied to a structure. The fatigue in

the structure can then be estimated using the cumulative statistics of these applied loads.

[0005] Piezoelectric transducers not only provide a mechanism for sensing fatigue in a structure but also can be used for self-powering of the sensors. Piezoelectric based self-powering for medical implants has several advantages over traditional battery powered techniques which suffer from limited life and complications due to biocompatibility. Poly-vinylidene diflouride (PVDF) is a piezoelectric plastic that is currently used for suture materials and has proven to be biocompatible. One disadvantage of PVDF is its very low mechano-electrical energy conversion. Such low power levels pose several challenges for designing self-powered sensors, which include:

1. Self-powered computation: Energy to perform sensing and computation on the sensor has to be harvested from the converted mechanical signal.

2. Non-volatile storage: All the parameters of internal state variables (intermediate and final) have to be stored on a non-volatile memory to account for unavailability of power (i.e. blackouts).

3. Sub-microwatt operation: All computation and storage functions have to be performed at sub-microwatt power dissipation levels to meet the power budget requirement of 1 μW.

[0006] Although many fatigue prediction algorithms mainly rely on the statistics of strain level crossings, it is well known that strain-rates experienced by a mechanical structure also play an important role in predicting fatigue. This is particularly important under high impact conditions during the usage of a biomechanical implant. Thus, it would beneficial to have a self-powered sensor capable of measuring the strain-rates experienced by a mechanical structure.

[0007] The statements in this section merely provide background information related to the present disclosure and may not constitute prior art.

SUMMARY

[0008] A self-powered sensor is provided for strain-rate monitoring and other low power requirement applications. The self-powered sensor is comprised of a piezoelectric transducer; a non-volatile memory comprised of at least one floating gate transistor; a current reference circuit adapted to receive a voltage signal from the piezoelectric transducer and operable to output a reference current into the non-volatile memory; an impact-monitoring circuit having a triggering circuit and a switch; the triggering circuit adapted to receive the voltage signal from the piezoelectric transducer and operable to control the switch based on the rate of change of the voltage signal.

[0009] Further areas of applicability will become apparent from the description provided herein. It should be understood that the description and specific examples are intended for purposes of illustration only and are not intended to limit the scope of the present disclosure.

DRAWINGS

[0010] Figure 1 is an exemplary S-N curve which can be used to estimate fatigue life;

[0011] Figure 2 is a system level architecture of an exemplary fatigue monitoring system;

[0012] Figure 3 is a simplified circuit model for a floating gate sensor;

[0013] Figure 4 is a graph of the read out current from a floating gate sensor over time;

[0014] Figure 5 is a schematic of an exemplary implementation of a floating gate sensor;

[0015] Figure 6 is a graph illustrating simulation results obtained using the floating gate sensor;

[0016] Figure 7 is a graph depicting the measured response of the single floating gate reference element;

[0017] Figure 8 is a system level architecture of an exemplary strain rate monitoring system;

[0018] Figure 9 is a simplified circuit model for a floating gate sensor;

[0019] Figure 10 is a schematic of an exemplary implementation of a strain rate sensor;

[0020] Figure 11 is a graph of a mathematical and measured responses of IHEI plotted on a logarithmic scale and a linear scale (inset);

[0021] Figure 12 is a graph of the injection responses for the impact with different rising speeds;

[0022] Figure 13 is a second graph of the injection responses for the impact with different rising speeds;

[0023] Figure 14 is a graph of measurements when a prototype sensor is subjected to different durations proportional to impact rate;

[0024] Figure 15 is a diagram of the system architecture for sensor;

[0025] Figure 16 is a diagram of a finite state machine employed by the sensor; and

[0026] Figure 17 is a graph of measurement for remote data acquisition.

[0027] The drawings described herein are for illustration purposes only and are not intended to limit the scope of the present disclosure in any way.

DETAILED DESCRIPTION

[0028] Mechanical fatigue is the accumulation of damage in a structure under applied fluctuating stresses. Though the magnitudes of the applied stresses are less than the tensile strength of the material, the progressive fatigue damage may lead ultimately to mechanical failure. Fatigue life is defined as the number of constant amplitude load cycles necessary to induce failure in an initially undamaged component. Generally, the fatigue life of a mechanical component under cycling applied load depends on the level of fluctuating strain in the structure. With reference to Figure 1, this can be represented by the S-N curve, which is obtained using experimental measurements. In the S-N curve, S is the mechanical strain level ($\Delta\varepsilon$) in the component under a harmonic load, and N is the number of cycles that causes failure of the component at that strain level.

[0029] The S-N curves can be used directly to estimate the fatigue life under constant amplitude harmonic load conditions. However, in most applications the applied load is not cyclic. The simplest approach to model fatigue behavior under variable amplitude load condition involves the concept of cumulative damage, which can be described using the Palmgren-Miner linear rule:

$$\sum_{i=1}^{m} \frac{n_i}{N_{fi}} = 1 \qquad (1)$$

where n_1 denotes total number of events when the electric signal generated by the piezoelectric transducer exceeded a threshold a_i. Miner's rule assumes that each strain cycle of a given magnitude consumes $1/N_{fi}$ of the total fatigue life, where N_{fi} is the fatigue life of the specimen at the given strain amplitude (obtained from the S-N curve). A major step in the implementation of this approach is the identification of different loading events that contribute to fatigue damage. Counting algorithms are used to reduce any loading spectra to a series of equivalent stress-strain states. The experimental data for each stress-strain

state is implemented with the Palmgren-Miner's rule to provide a summation of fatigue damage. Several empirical cycle counting methods have been developed for different applications. For the purpose of this study, a modified level-crossing peak counting method is used. This method consists of detecting and summing the maximum level reached by different peaks of the applied strain function. It is readily understood that other counting methods may be employed.

[0030] Figure 2 illustrates a system level architecture of an exemplary fatigue monitoring system 20. The fatigue monitoring system 20 is comprised of a piezoelectric transducer 22, a rectifier 24 and a floating gate sensor 26. The piezoelectric transducer 22 may be operably coupled to a structure being monitored, such as a medical implant. Stress applied to the monitored object causes the piezoelectric transducer 22 to generate a voltage signal While reference is made throughout this disclosure to medical implants, it is readily understood that the fatigue monitoring system has other applications (e.g., monitoring structural integrity of aircraft or vehicle components).

[0031] The floating gate sensor 26 continuously records the output of the piezoelectric transducer 22. The full-wave rectifier 24 interposed between the piezoelectric transducer 22 and the floating gate sensor 26 generates un-regulated supply voltages (vdd and gnd) from the signal output by the transducer 22. In an exemplary embodiment, the full wave rectifier 24 is implemented using a standard diode bridge. For the prototype described below, n+ - p-substrate and p+ - n-well diodes were used, which naturally occur using electrostatic discharge (ESD) diodes. The supply voltages are used by a floating gate sensor 26 to compute the amplitude and duration statistics of the rectified signal. The floating gate sensor 26 then updates the internal variables which represent cumulative history of the mechanical strain cycles experienced by the monitored structure. The floating gate sensor is self-powered and extracts all its operational energy from the rectified signal.

[0032] The floating gate sensor 26 may interface an RFID sensor 30 that is used to interrogate and/or download the recorded statistics. The RFID sensor 30 embeds a classifier 32 that uses the statistics as features to produce a

confidence value proportional to time-to-failure. An RFID interface 34 is then used to transmit the confidence value to an external interrogator. The powering and operation of the RFID-subsystem is completely asynchronous and derives its power through RF coupling from an external interrogator.

[0033] A simplified circuit model for the proposed floating gate sensor 22 is shown in Figure 3. It consists of a floating gate (denoted by voltage V_g) which is coupled to the gates of an injection transistor M1 and a read-out transistor M2. The current delivered by the piezoelectric transducer is limited by a current reference (I_0) which biases the transistor M1 in weak-inversion. The nodes C and T represent control and tunneling terminals. In weak-inversion, the expression for source current through the pFET transistor M1 is given by:

$$I_0 = I_s e^{-\kappa \frac{V_g}{U_T}} e^{\frac{Vs}{U_T}}$$

where I_0 is the source current, I_s is a pre-exponential current, V_g is the floating gate voltage, κ is the coupling coefficient from floating gate to channel, U_t is the thermal voltage. For the fixed reference current I_0, the gate current of M1 due to impact ionized hot-electron injection (IHEI) is given by:

$$I_g = \beta I_0 e^{\frac{V_s}{V_{inj}}} = -C\frac{\partial V_g}{\partial t}$$

where β and V_{inj} are constants, and C is the total capacitance at the floating gate. Using equations (1) and (2), the following expression for V_g is obtained as a function of

time:

$$V_g(t) = -\frac{1}{K_2}\log\left(K_1K_2\left(t + \frac{1}{K_1K_2}e^{-K_2V_{g0}}\right)\right)$$

where

$$K_1 = \left(\frac{\beta I_0}{C}\right)\left(\frac{I_0}{I_s}\right)^{\frac{U_t}{V_{inj}}}$$

$$K_2 = \frac{\kappa}{V_{inj}}$$

and V_{g0} is the initial gate voltage.

The floating gate voltage is mapped onto a read-out current I_{out} using the transistor M2. Because transistor M2 may not be in a weak-inversion we use an EKV model to compute the output current I_{out} as:

$$I_{out} = a^2 \log^2\left(1 + \alpha e^{\frac{-\kappa V_g + V_B}{U_T}}\right)$$

where α and a are parameters of the model. Figure 4 plots the read-out current I_{out} over time for parameters a and α, obtained experimentally. It can be seen from the model that the response of the circuit is monotonic and exhibits a saturating response. Therefore the model in Figure 3 could be used for calculating the total cumulative time a piezoelectric-transducer was able to deliver a load of current I_0, which will be proportional to the cumulative stress period applied to the implant.

[0034] Figure 5 illustrates an exemplary implementation of a floating gate sensor 50. The floating gate sensor 50 is comprised of a current reference circuit 52, a driving circuit 54 and a storage circuit 56. Each of these circuits is further described below.

[0035] In an exemplary embodiment, the reference current circuit 52 is implemented using transistors T1-T5 and resistor R. In a standard current reference circuit, the ratio of the pMOS current mirror transistors along with R determines the magnitude of the reference current. This exemplary implementation uses a floating gate transistor T2 coupled to a gate of

transistor T1. The reference current is determined by the charge injected onto the floating gate T2 and the resistor value R. When all the transistors T2-T5 are biased in weak-inversion (i.e., operating in a sub-threshold mode), the reference current through T4 is given by

$$I_{ref} \approx \frac{Q_f}{C_f R}$$

where Q_f is the charge stored on the floating gate C1 and C_f is the total floating gate capacitance. By accurately controlling the amount of floating gate charge, Q_f, small increments of reference current can be generated. The charge on the gate can be modified using hot electron injection or through tunneling. Injection adds electrons to the floating gate as a result its potential decreases which leads to an increase in the drain current through the transistor. For a pMOS transistor biased in weak-inversion drain-to-source voltages greater than 4.5V has been found to be sufficient for injection. Of note, the current reference circuit is able to compensate for temperature variations, as evident from reference current expression which is independent of temperature dependent parameters. Temperature compensation due to the current reference circuit has been validated through simulation and exhibits less than 2% variation over a 70°C variation in temperature. Even though this feature is not required during normal operation of the implantable device, it has been observed that for some implants (hip implants) repeated wear and tear can dramatically increase in ambient temperature. While a particular circuit configuration was described above, it is readily understood that other circuit configurations, preferably having at least one floating gate transistor, may be used for the current reference circuit.

[0036] In the exemplary embodiment, a storage capacitor C_a was used at the output of the rectifier to filter out unwanted high-frequency components. The size of the capacitor provides a trade-off between total discharge time versus the voltage swing at the sensor. For the prototype an external capacitor (10nF) was chosen which led to voltage swing of up to 8V for 20V generated by the piezoelectric transducer. A voltage over-protection and

clamping circuitry was integrated at the output of the diode bridge to prevent damage due to unwanted piezoelectric surges.

[0037] The storage circuit 56 is an array of floating gate transistors C2-C6 which provide non-volatile storage. A floating gate is a poly-silicon gate surrounded by an insulator, which in standard semiconductor fabrication process is silicon-dioxide. Because a floating gate is surrounded by high quality insulation any electrical charge injected onto this gate is retained for long intervals of time (> 8 years). In the exemplary embodiment, each floating gate transistor C2-C6 also has a tunneling capacitor which is used for removing electrons (erase operation) from the gate. It is envisioned that other types of storage circuits are within the broader aspects of this disclosure.

[0038] An exemplary driving circuit 54 is interposed between the current reference circuit 52 and the array of floating gate transistors 56. In this exemplary circuit, transistors T7-T12 mirror the current in T4 to drive the floating gate transistors C2-C7. More specifically, the driving circuit is comprised of a plurality of circuit branches, where each circuit branch electrically couples to a different floating gate transistor in the array of floating gate transistors. Voltage drop in each branch will be controlled using diode connected pMOS transistors and will ensure different drain-to-source voltage across each of floating gate cells C2-C7. During the pre-calibration stage each of the floating gate cells are programmed (using tunneling and injection) to store a fixed amount of charge, hence a fixed gate voltage across C2-C7. When a rectified voltage is presented across the supply terminals (+-), the circuit generates a reference current and a stable voltage reference at node Vc. Depending on the magnitude of the rectified voltage, different cells C2-C7 start injecting charge on its floating gate. Likewise, other circuit configurations are envisioned for the driving circuit.

[0039] SpectreS based spice simulation of the current reference circuit demonstrates an activation profile of different floating gate cells C2-C7 at different peak amplitude as show in Figure 6. For this experiment a storage capacitor of 10nF was chosen, and the duration of the piezoelectric pulse excitation was set to 2 seconds. The circuit exhibits a start-up time of 100ms,

which is sufficient for most structural engineering applications. The start-up however can be optimized by appropriately sizing the storage capacitor at the rectifier but at the expense of lower coupling voltage (rectifier). The simulation also shows poor current regulation of the reference circuit due to sub-threshold operation of the circuit but does not adversely affect the response of the sensor.

[0040] The results indicate that different floating gate cells in the array start injecting at different piezoelectric potential and therefore record cumulative amplitude statistics of a signal. The architecture therefore implements a self-powered flash data converter. The total charge accumulated on the floating gate is measured by sensing the current through the read-out transistors T13-T18. The transistors T13-T18 act as read-out transistors that are used to quantify the stored charge on floating gates C2-C7 by measuring the drain currents flowing through T13-T18. The read-out transistors are powered by an external interrogator by transferring energy via physical inter-connections or via RF coupling. Thus, the sub-circuit enclosed in the dotted line in Figure 5 is to be implemented in the RFID sensor subsystem in Figure 2. The drain currents through transistors T13-T18 represents a feature vector encoding the history of stress-strain patterns and is used by a classifier to generate time-to fail confidence scores.

[0041] A prototype floating-gate sensor was fabricated in a standard 0.5μm CMOS process. The floating gate transistors were designed using a double polysilicon transistor with a minimum injection potential of 4.2V and an erase voltage of 15V. For preliminary experiments, a signal generator was used to simulate the functionality of a piezoelectric transducer. Different voltage levels were applied at the floating gate array input and the read-out current through transistor T13 was measured.

[0042] Figure 7 shows the current measured through transistor T13 for different voltages against the total duration of the applied input. The injection profiles for different voltages are relatively close to each other due to current reference based injection architecture. The response is monotonic and approximately linear which demonstrates that the sensor can be used for

computing total strain cycles experienced by a mechanical structure. The total power dissipated during the entire experiment was measured to be 320nW which is well below the power generated by a PVDF transducer (1μW). For long term monitoring it is critical that the measured current show a compressive non-saturating response (equivalent to logarithmic response). Long term monitoring experiments with the floating gate sensor have shown non-saturating response for up to 10^5 seconds demonstrating the effectiveness of current limiting transistors T7 in Figure 5.

[0043] In this disclosure, embodiments of a self-powered fatigue measuring system based on a combination of piezoelectric transduction and floating gate injection was demonstrated. Preliminary results indicate that the response of the sensor is proportional to an equivalent total number of stress cycles experienced by a structure. The total power dissipation of the sensor is less than 1μW. The above description is merely exemplary in nature and is not intended to limit the present disclosure, application, or uses.

[0044] In a second embodiment, the circuitry of a fatigue monitoring circuit may be modified so that the self-powered sensor can act as a long term strain rate monitor. Although many fatigue prediction algorithms mainly rely on the statistics of strain level crossings, it is well known that strain-rates experienced by a mechanical structure also play an important role in predicting fatigue. This is particularly important under high impact conditions during the usage of a biomechanical implant. In the following embodiment, a self-powered sensor capable of reporting statistics of the rate of the strain change inside a given structure is described. Although the internal circuitry differs from the sensor described above, the framework is similar to that described above, as power is harvested using the strain on a given piezoelectric transducer and strain rate statistics are recorded using the harvested energy.

[0045] As described above, the sensor directly harvests power from the strain itself. This is challenging because a piezoelectric transducer only generates nanowatts of power. The proposed circuitry allows the sensor to operate on the relatively small amount of power harvested from the

piezoelectric transducer.

[0046] Figure 8 illustrates a system level architecture of an exemplary long term strain rate monitoring sensor. The strain rate monitoring sensor is comprised of a piezoelectric transducer 120, a startup circuit 122, a reference circuit 124, an impact rate monitoring circuit 126 and a non-volatile memory 128. The piezoelectric transducer 120 may be operably coupled to a structure being monitored, such as a medical implant. Stress applied to the monitored object causes the piezoelectric transducer 120 to generate a voltage signal. As the stress varies, the voltage signal varies accordingly. The rate at which the voltage signal varies is, therefore, proportional to the rate at which strain is applied to the sensor varies. Thus, the strain rate monitoring sensor measures strain rate statistics by measuring the rates at which the voltage signal varies. The floating gate sensor may interface an RFID sensor (not shown) or another device that is used to interrogate and/or download the recorded statistics, details of which are described above. While reference is made throughout this disclosure to medical implants, it is readily understood that the fatigue monitoring system has other applications (e.g., monitoring structural integrity of aircraft or vehicle components).

[0047] Strain rate monitoring sensor continuously measures the rate of strain placed on piezoelectric transducer 120. As the amount of strain placed on piezoelectric transducer 120 varies, the voltage produced by transducer 120 will also vary. As the voltage signal varies, startup circuit 122 enables the reference circuit to generate a reference current having stable state. Reference circuit 124 mirrors the stable reference current and supplies the reference current to impact rate monitoring circuit 126. The impact rate monitoring circuit is designed such that when the frequency of the voltage signal exceeds a certain threshold, a triggering circuit drives a switch in the impact rate monitoring circuit, which allows the reference current to flow from reference circuit 124 to the non-volatile memory 128, which continuously injects electrons or charge into a floating gate transistor for as long as the switch is closed. Once the rate of change decreases below the predefined frequency, the injector is

once again starved of current and the injection process ends. The total amount of time that the strain rate exceeds a predetermined threshold is proportional to the amount of electrons or charge stored in non-volatile memory 128.

[0048] The operation of the proposed impact rate monitor is illustrated using the schematic shown in Fig. 9. It consists of the current starved floating-gate injection circuit FG that was discussed above. The circuit consists of a pMOS floating-gate transistor M_p which is connected to a constant current source I_S. The gate of transistor V_{FG} is completely insulated by silicon-di-oxide. Thus, the floating-gate injection circuit acts as a non-volatile memory. As a result, electrons injected onto the node are retained for a long period of time. For impact-rate monitoring, triggering circuit TC controls a switch SW which allows the reference current I_S, to flow through the injector. When the voltage generated by the piezoelectric transducer is sufficiently high (typically > 4.2V in a 0.5um CMOS process), and the switch is ON, IHEI starts and electrons are injected onto the floating-gate.

[0049] Figure 10 depicts an exemplary embodiment of the schematic of the impact rate monitor 130. Impact rate monitor is comprised of a piezoelectric transducer (not shown), startup circuit 130, reference circuit 132, and at least one impact monitoring circuit 134A-134C.

[0050] When a strain or force is exerted on the piezoelectric transducer of the impact rate monitor, startup circuit 130 initializes reference circuit 132 whereby the reference current flowing from reference circuit 132 jumps from one stable point, $I_{rc} = 0$, to a second stable point, where I_{rc} is equal to some constant value, independent of voltage. Put another way, the current reference circuit has two stable states, one state where the reference circuit 132 conducts no current and a second stable state where the reference circuit conducts a reference current. Startup circuit 130 is implemented so that the reference circuit is always in one of the two states. The drain of transistor S1 is connected to V_+ and V_- is connected to the gate of transistor S1. Capacitor C0 is connected to the source of transistor S1. The intermediate node between capacitor C0 and transistor S1 is the gate of S2. Exemplary startup circuit 130 is

comprised of two p-type transistors S1 and S2 and capacitor C0. Thus, when the piezoelectric transducer produces a voltage potential and power is available, transistor S1 is on and will charge C0 until C0 is charged. While C0 is charging, S2 will drive the gate of M3 by injecting additional current at the startup. Once C0 is charged, then startup circuit 130 is switched off.

[0051] Reference circuit 132 can be a standard reference circuit. Reference circuit 132 is comprised of two current mirrors, the first current mirror is comprised of transistors M1 and M5 and the second current mirror is comprised of transistors M4 and M8. The reference current is determined by the size of transistor M1 and M5 (e.g. M1 = 60μm/10μm, M5 = 30μm/10μm) and the value of resistor RF (e.g. 1.5MΩ). Transistors M3 and M7 and transistors M2 and M6 may be optionally used to improve the performance of the reference circuit 132. The reference circuit 132 supplies current to the floating gate injectors F1-F3 of the impact monitoring circuits 134A-134C. It is understood that the above-described reference circuit is merely an exemplary embodiment and that a number of alternative embodiments may be used as a reference circuit.

[0052] Exemplary impact monitoring circuits 134A-134C consist of current copiers P1 and P2, P3 and P4, P5 and P6, P7 and P8, P9 and P10, and P11 and P12, a triggering circuit 136A-136C for each impact monitoring circuit 134A-134C, and a floating gate injection circuit FC connected to each triggering circuit and operable to receive a reference current from current copiers P3 and P4, P5 and P6, and P11 and P12. Each current copier P1-P12 is comprised of two p-type transistors receiving the reference current from the current mirror of reference circuit 132. The current copiers are used to provide the amplifiers N1-N3 and floating gate injectors 138A-138C with identical currents corresponding to the reference current. It is understood to those having skill in the art that alternative embodiments of current copiers exist and may be used interchangeably.

[0053] The triggering circuits 136A-136C are individually compromised of a high-pass filter formed by resistor R and capacitor C-3C

(commonly referred to as an R-C bridge), common source amplifiers N1-N3 connected at the intermediate nodes of the R-C bridges, and switches SW1-SW3.

[0054] The impact monitoring circuits 134A-134C are configured such that impact monitoring circuits 134A-134C may begin receiving current at different rates. While Fig. 10 depicts an embodiment having three impact monitoring circuits channels134A-134C, it is understood that a self-powered circuit may have more or less than three impact monitoring circuit channels. Each triggering circuit 136A-136C has a high-pass filter operable to filter out a specific frequency. When the rate of change of the voltage signal produced by the piezoelectric transducer exceeds a predetermined threshold, current will flow from V+ and V- through the high pass filter, thereby biasing the gate of a common source amplifier N1-N3. By choosing capacitors C-3C with different capacitances (e.g. 5, 10 and 15 nF respectively), each high-pass filter will begin operating at a different frequency (10Hz, 5Hz and 2.5Hz respectively). Capacitors C-3C for the triggering circuits are all located off-chip due to their relatively large size. Common source amplifiers N1-N3 are n-type transistors that serve as comparators and operate to drive switches SW1-SW3. The sources of common sources of amplifiers N1-N3 are connected to the current copiers and their drains are connected to V-. Unlike the high-pass filters, which do not receive the reference current, the common source amplifiers N1-N3 receive a reference current when the gate of the amplifier is sufficiently biased. When a high-pass filter receives a sufficient voltage signal, current flows from V+ to V- via the high pass filter. The current flowing through the high-pass filter biases the gate of common source amplifier N1-N3, which drives a switch SW1-SW3. Switches SW1-SW3 are p-type transistors that allow the reference current to flow to the floating gate injection circuit 138A-138C when switch SW1-SW3 is closed. It is envisioned that alternative embodiments of the triggering circuit may be used in building the disclosed self-powered strain-rate sensor.

[0055] Once the switch is closed, a charge may be injected into floating gate injection circuit 138A-138C, which may be comprised of transistors

F1-F3 and capacitors C1-C3. The floating gate injection circuit 138A-138C is a storage circuit. The charge is supplied by the reference current received from reference circuit 132. Floating gate injection circuits 138A-138C are collectively an array of floating gate transistors which provide non-volatile storage. A floating gate is a poly-silicon gate surrounded by an insulator, which in standard semiconductor fabrication process is silicon-dioxide. Because a floating gate is surrounded by high quality insulation any electrical charge injected onto this gate is retained for long intervals of time (> 8 years). In the exemplary embodiment, each floating gate transistor also has a tunneling capacitor C1-C3 which is used for removing electrons (erase operation) from the gate. The floating gate injectors are operating in weak-inversion mode. The presented floating injection circuit is merely an exemplary embodiment. It is envisioned that other types of storage circuits are within the broader aspects of this disclosure.

[0056] If T denotes the set of time intervals during which the triggering is enabled, then the source voltage V_s, can then be expressed as

$$V_s = \frac{1}{K_2}\log\left(K_1 K_2 \int \partial\tau + e^{-K2V_{SO}}\right) \qquad (1)$$

with

$$K_1 = \frac{\kappa\beta I_S}{C_t}, K_2 = \frac{1}{V_{inj}}$$

where K is the floating-gate efficiency, C_1 is the total capacitance of node V_{FG}, β and V_{inj} are injection parameters which only depend on the aspect ratio of the transistor and the CMOS process. Figure 11 plots the voltage V_s, according to equation (1) with respect to the total triggering duration and compares it with measured result obtained from a fabricated prototype in a 0.5-.µm CMOS process. The measured response is shown to be in close agreement with the mathematical model in equation (1). Under the condition when the total triggering duration satisfies $\int_{t\in T} d\tau << e^{K_2 V_{SO}} / K_1 K_2$, a linear response of V_s with respect to t is obtained. This region is highlighted in the Fig. 12 inset and is

useful for short-term monitoring. For the condition $\int_{\tau \in T} d\tau >> e^{K_2 V_{fg}} / K_1 K_2$, equation (1) can be approximated by a log-linear response as:

$$V_s = -\frac{1}{K_2}\log(K_1 K_2) - \frac{1}{K_2}\log\left(\int \partial\tau\right) \quad (2)$$

where τ ε T.

[0057] The log-linear response shown in Fig. 2 is important for long-term impact monitoring applications. The first part of equation (2), $-\frac{1}{K_2}\log(K_1 K_2)$, denotes an offset which is dependent on biasing and initialization conditions, where as the second part in equation (2), $-\frac{1}{K_2}\log\left(\int \partial\tau\right)$ is a log-linear function of the total triggering duration and is scaled by the parameter K_2.

[0058] The floating-gate injectors have a robust response to mismatch and variations in biasing conditions. For instance, the variation in the parameter K_2, was measured to be less than 10% when the bias current was varied by more than 100%. This result is encouraging because it implies that the precision of the source current is not critical for the operation of the injector. The variation in the parameter K_2 for different injectors (located on different silicon dies but from the some fabrication run) was found to be less than 15%. Thus, by operating the injector in a differential manner, the offset in equation (2) can be eliminated where the response can be expressed only as a function of K_2 and the total triggering duration as:

$$V_S = \frac{1}{K_2}\log\left(\frac{t_0 + \partial\tau}{t_0}\right)$$

where t_o denotes a reference time with respect to which the triggering duration is measured.

[0059] Before the sensor can be used for monitoring, all the outputs of the floating-gate injectors (01-03) are first equalized to the same potential. The equalization procedure is similar to the method presented above, where an

injector to be initialized is first selected. The input terminals V^+ and V^- are then connected to 5.5V and the floating-gate transistor is injected till the output voltage 01-03 reaches 4.8V. This potential is sufficient to initiate an IHEI process when the channel is triggered by enabling the switches SW1- SW3.

[0060] When the voltage level produced by the piezoelectric transducer exceeds a threshold voltage (3.3V), reference circuit 132 initializes all the current biases. For the circuit in Fig. 10 and parameters given in Table 1, the startup time for the current reference is 30ms. The startup time determines the upper bound of the impact rates that can be measured using the sensor. This was found to be <35Hz which is within the range of most biomechanical impact rates (1 Hz-50Hz). Based on the rate of change of the supply voltages V^+ and V^-, the bandwidth of the high-pass filter determines the amplitude of the signal presented at the input of the comparator N1. When the signal amplitude exceeds the threshold of the comparator (determined by the bias current), the switches SWI-SW2 are triggered (active "low") and as a consequence the injectors F1 and F2 record the occurrence of the impact. Figure 12 shows the AC response of the filters whose low-frequency cut-offs have been set to 10Hz, 5Hz and 2.5Hz. This ensures that impact monitor circuit IMC1 triggers only for a slow varying input signal (slowly changing impact). However, all the impact monitor circuits 134A-134C trigger for a fast varying input signal (high impact rates). Fig. 13 shows the triggering event for the three impact monitor circuits, when channel 1 is not triggered where as channel 2 and 3 are triggered. Note that the duration of the triggering is different for channel 2 and 3 implying that channel 3 will inject for a longer duration compared to channel 2.

[0061] Even though the floating-gate injectors are equalized by programming the output voltage 01-03 to 4.8V, the procedure is still prone to initialization errors. We compensate for these errors by using a calibration procedure based on the differential response of the injector as given by equation (3). All the channels are first allowed to inject for a reference duration t_o such that $t_o >> e^{K_2 V_{fg}} / K_1 K_2$. This ensures that the initialization errors and biasing errors are fully calibrated before the sensor is used for monitoring. Fig. 14 shows the calibration procedure where all the three channels are injected for a duration of

$t_0 = 3000s$. It can be seen that at the end of 3000 cycles, the initialization errors for all the three channels have been calibrated.

[0062] After the calibration procedure, the fabricated prototype was subjected to different impact rates which were synthetically generated using a programmable signal generator. An equivalent input voltage (emulating the transducer output) to the prototype was 6.1 V. The impact rates (based on the RC time-constant) were chosen such that channel I did not inject, where as channel 2 injected for only 85^0/a of the duration and channel 3 injected for 100% of the duration. Fig. 14 shows that the sensor is able to distinguish different impact-rate levels, where the offset in the log-linear response is directly proportional to the relative triggering duration (calculated with respect to the total observation period). Even though Fig. 14 shows the operation of the sensor up to 40000 cycles (seconds), we have verified its functionality beyond 10^5 cycles.

[0063] The embodiment described above describes a nanowatt integrated circuit that can harvest power from a piezoelectric transducer to monitor strain rates experienced by a structure. The sensor is based on a novel integration of a triggering circuit with a piezoelectric-floating gate injector and can operate for more than 1,000,000 load cycles. The sensor integrates computation and storage within a single device that can have a size of 1.5mm x 1.5mm and can be imbedded inside structures for autonomous monitoring and fatigue sensing. The above description is merely exemplary in nature and is not intended to limit the present disclosure, application, or uses.

[0064] In an alternative embodiment, the piezoelectric transducer may be in the form of a piezoelectric film. The piezoelectric film may be connected to the circuitry presented above. The piezoelectric film may be configured to fit on a tamperproof cap or packaging so that tampering may be detected even in the absence of a seal being broken.

[0065] One additional feature of the sensor is the ability to remotely calibrate and read the information stored in the sensor. Because the sensor is self-powered and the energy harvested from the piezoelectric transducer can only be used for hot-electron injection; the power for remote interrogation using radio-frequency waves has to be supplied by a remote reader. The energy

delivered to the sensor has to be enough to operate high-voltage charge pumps, operate analog-to-digital converters, data encoding circuits, state-machines and analog frontend circuits. Remote calibration is important for successful and mass deployment of sensors in an embedded manner.

[0066] The method to remotely calibrate the floating-gate sensor is described below. A FSM (Finite State Machine) is implemented in the sensor together with the floating-gate array. Controlled by the FSM, the on-chip charge-pump can generate the required voltage for programming and the A/D converter can sample data which are stored in the floating-gate transistor. Moreover, the MODEM (Modulator and DEModulator) performs the wireless communication between the sensor and remote device which facilitates the calibration procedure.

[0067] The system architecture of the sensor is depicted in Figure 15. The wireless telemetry between the sensor and remote device is based on the inductive coupled mechanism. In the receiving path, “Antenna” coil picks the RF (Radio Frequency) signal in the field. When a specific command is sent by ASK (Amplitude Shift Key) modulation, “Demodulator” senses the amplitude variation of carrier and decodes a valid command (cmd1 to cmd6). Once “FSM” receives the valid command, different control signal is generated to enable/disable “Charge-pump” or “A/D converter.” In the transmitting path, after the data in “Floating-gate array” are sampled, the digital-formed data are encoded (e.g. Manchester code) and transmitted through “Modulator” by load impedance modulation. The descriptions of each building blocks are summarized in Table 1 below.

Table 1: Descriptions of building blocks

Block	Function
Modulator & Demodulator	RF front-end, decrypts valid command and encodes sampled data
FSM	control block for remote calibration
Charge-pump	on-chip high voltage generator for FN tunneling
A/D converter	data conversion from analog form to digital pattern
Floating-gate array	sub-microwatt analog processor for long-term strain monitor

[0068] Assume a 7-channel floating-gate array has been implemented in the sensor, among which 4 channels are used for magnitude monitoring and 3 channels for the impact-rate. The remote calibration procedure controlled by "FSM" is performed as following:

1) the residual voltage (random after fabrication) for the current channel is acquired by cmd5, the sampled data are sent by through "Modulator";
2) if the voltage is higher than V_0 (starting voltage for all the channels), cmd4 is sent to trigger the hot electron injection; after a small period of time, cmd4 is sent again to stop the injection; if the voltage is lower than V_0, cmd3 is sent to enable "Charge pump" for FN tunneling; after a small period of time, cmd3 is sent again to disable "Charge pump";
3) the residual voltage for the current channel is acquired again by cmd5;
4) repeat step 2) if the residual voltage is not equal to V_0, otherwise sent cmd2 to shift to the next channel for calibration.

[0069] After the calibration of all the 7 channels, the sensor can be used for long-term strain monitoring. When the resultant data are required, cmd5 or cmd6 can be used for single data acquisition or continuous data acquisition. Note cmd1 is only reserved for testing. The state machine for "FSM: is diagrammed in Figure 16 and the detail descriptions of each state are listed in Table 2 below.

Table 2: Descriptions of FSM states

State	Descriptions
S_0	Idle state – wait for new command
S_1	Test state – send back specific data frame for testing
S_2	Channel selection state – shift to the next available channel for data acquisition
S_3	Tunneling state – enable/disable the on-chip charge pump for tunneling
S_4	Injection state – enable/disable the trigger for hot electron injection
S_5	Single acquisition state – sample and send back the data from current channel
S_6	Continuous acquisition state – sample and send back the data from current channel and shift to the next channel (repeat)

[0070] The proposed remote-calibration method has been implemented with the sensor in a 0.5-μm standard CMOS process. The measurement result for one example command is presented in Figure 17. For sending the command, 100% ASK modulation is used and the envelope variation of the RF signal is denoted as Channel 4. After the command is decrypted by "Demodulator," the valid command in PWM (Pulse Width Modulation) is shown as Channel 3. In this example, cmd5 is sent and the sensor starts to sample the current floating-gate channel by A/D converter. Afterward, the data are encoded into serial Manchester code and sent back to remote device as indicated by Channel 2. Channel 1 is the variation of the RF envelope detected from the remote device which shows the data in both receiving and transmitting path. The experiment indicates the correct function for the remote access to the sensor.

[0071] Thus the procedure of the remote-calibration of the piezo-floating-gate transistor is described above. Controlled by "FSM", the sensor is able to respond to various commands and to perform the required manipulations remotely. Consequently, it becomes more convenient to access the sensor when integrated with such additional feature, and it also greatly expands the potential applications for the long-term fatigue monitoring.

[0072] The foregoing description of the embodiments has been provided for purposes of illustration and description. It is not intended to be exhaustive or to limit the invention. Individual elements or features of a

particular embodiment are generally not limited to that particular embodiment, but, where applicable, are interchangeable and can be used in a selected embodiment, even if not specifically shown or described. The same may also be varied in many ways. Such variations are not to be regarded as a departure from the invention, and all such modifications are intended to be included within the scope of the invention.

CLAIMS

What is claimed is:

1. A self-powered sensor comprising:

a piezoelectric transducer;

a non-volatile memory

a reference circuit, the reference circuit adapted to receive a voltage signal having rate of change from the piezoelectric transducer and operable to output the reference current into the memory;

an impact rate monitoring circuit including a switch and a triggering circuit;

the switch interposed between the reference circuit and the memory; and

the triggering circuit adapted to receive the voltage signal from the piezoelectric transducer and operable to control the switch based on the rate of change of the voltage signal.

2. The self-powered sensor of claim 1 wherein the triggering circuit is operable to close the switch when the rate of change of the voltage signal exceeds a predefined threshold.

3. The self-powered sensor of claim 1 wherein the triggering circuit includes a high-pass filter sensitive to the rate of change of the voltage signal.

4. The self-powered sensor of claim 3 wherein the triggering circuit further comprises an amplifier interposed between the high-pass filter and the switch.

5. The self-powered sensor of claim 4 wherein the amplifier is configured as a comparator and is operable to drive the switch when the high-pass filter determines that the voltage signal has exceeded the predefined threshold.

6. The self-powered sensor of claim 1 wherein the piezoelectric transducer is operable to power the self-powered sensor.

7. The self-powered sensor of claim 1 wherein the non-volatile memory is comprised of an array of floating gate transistors.

8. The self-powered sensor of claim 7 wherein the reference circuit is operable to inject a charge onto different floating gate transistors of the array based on the rate of change of the voltage signal.

9. The self-powered sensor of claim 8 wherein the impact monitoring circuit is comprised of a plurality of channel circuits, where each channel circuit is operable to inject a charge into different floating gate transistors of the array based on the rate of change of the voltage signal.

10. The self-powered sensor of claim 9 wherein each circuit branch defines a different voltage rate threshold, whereby charge is injected into the floating gate transistor associated with a given channel circuit when the magnitude of the reference current exceeds the voltage change rate threshold for a given channel circuit.

11. The self-powered sensor of claim 1 further comprising a startup circuit interposed between the piezoelectric transducer and the current reference circuit.

12. The self-powered sensor of claim 11 wherein the startup circuit is operable to receive a voltage signal and to cause the reference circuit to generate a stable reference current.

13. The self-powered sensor of claim 9 wherein each channel circuit is further comprised of a current copier operable to receive the reference circuit and to supply the triggering circuit and the switch with the reference current.

14. The self-powered sensor of claim 1 wherein the piezoelectric transducer is operably coupled to a medical implant, such that the voltage signal is

generated by the piezoelectric transducer when the piezoelectric transducer experiences a change in strain.

15. The self-powered sensor of claim 14 wherein the total charge stored the non-volatile memory corresponds to the amount of time the rate of strain exceeds a predefined threshold.

16. A self-powered sensor comprising:

a piezoelectric transducer operable to produce a voltage signal corresponding to a change of rate of strain exerted on the piezoelectric transducer;

a startup circuit operable to receive the voltage signal produced by the piezoelectric transducer and to supply a current to a reference circuit;

the reference circuit operable to receive a current from the startup circuit, to generate a stable reference current and to mirror and supply the reference current to an impact monitoring circuit;

the impact monitoring circuit comprising a plurality of impact monitoring channel circuits, each impact monitoring channel circuit sensitive to a predefined frequency corresponding to a rate of change in the voltage signal;

each impact monitoring channel circuit operable to supply the reference current to a corresponding floating gate injector when the impact monitor channel circuit senses a frequency exceeding the predetermined frequency threshold; and

each floating gate injector operable to inject charge into a floating gate transistor while the frequency of the voltage signal exceeds the predefined frequency threshold.

17. The self-powered sensor of claim 16 wherein each impact monitoring channel circuit further comprises a triggering circuit and a switch, the triggering circuit operable to drive the switch when the frequency of the voltage signal exceeds the predefined frequency threshold.

18. The self-powered sensor of claim 17 wherein the triggering circuit further comprises a high-pass filter operable to detect a frequency of the voltage signal that exceeds the predefined frequency threshold and operable to bias the gate of a common-source amplifier, the common-source amplifier operable to drive the switch when the gate of the common-source amplifier is biased.

19. The self-powered sensor of 18 wherein the impact monitoring channel circuit further comprises a first current copier and a second current copier;

the first current copier operable to receive the reference current and to supply the reference current to the common source amplifier;

the second current copier operable to receive the reference current and to supply the reference current to the floating gate injector.

20. The self-powered sensor of 18 further comprising a plurality of voltage nodes, each node corresponding to a impact rate channel circuit and each node having a charge corresponding to the charged stored in a capacitor in the floating gate capacitor.

21. A self-powered device for gathering statistics on strain rate comprising:

a transducer operable to generate a voltage signal in response to mechanical stress;

a reference circuit operable to receive said voltage signal and generate a stable reference current;

an impact monitoring circuit operable to receive the voltage signal and the reference current when the frequency of the voltage signal exceeds a predetermined threshold; and

the impact monitoring circuit operable to inject a charge into a non-volatile memory when the frequency of the voltage signal exceeds said predetermined threshold.

22. The self-powered device of claim 21 wherein the impact rate monitoring circuit further comprises a triggering circuit operable to determine when the

frequency of the voltage signal exceeds the predetermined threshold and to inject charge into said memory when the voltage signal exceeds the predetermined threshold.

23. The self-powered device of claim 22 wherein the triggering circuit further comprises a high pass-filter operable to receive the voltage signal and to bias the gate of a common source amplifier when said the frequency of the voltage signal exceeds a predetermined threshold.

24. The self-powered device of claim 23 wherein the triggering circuit further comprises a switch that is driven by the common-source amplifier when the voltage signal exceeds a predetermined threshold and operable to allow the reference current to flow to the memory when said switch is closed.

25. The self-powered device of claim 21 wherein said device is operable to interface with an RFID chip, whereby statistics relating to strain may be uploaded by a user and the device can be remotely calibrated and configured.

26. A self-powered sensor comprised of:

a piezoelectric transducer operable to generate a voltage signal;

a non-volatile memory operable to store statistics of strain rate and strain level;

a means for injecting a charge into said memory when a rate of strain exceeds a predetermined threshold;

a means for injecting a charge into said memory when a level of strain exceeds a predetermined threshold

27. A device for measuring the rate of strain applied to a tamperproof cap comprising:

a piezoelectric film sized to fit on a tamperproof cap and operable to generate a voltage signal corresponding to the rate of strain applied to the tamperproof cap;

a reference circuit operable to receive the voltage signal from said film and operable to generate a reference current;

a impact monitoring circuit operable to receive the voltage signal and the reference current and to inject charge into a non-volatile memory when said the frequency of said voltage signal exceeds a predetermined threshold.

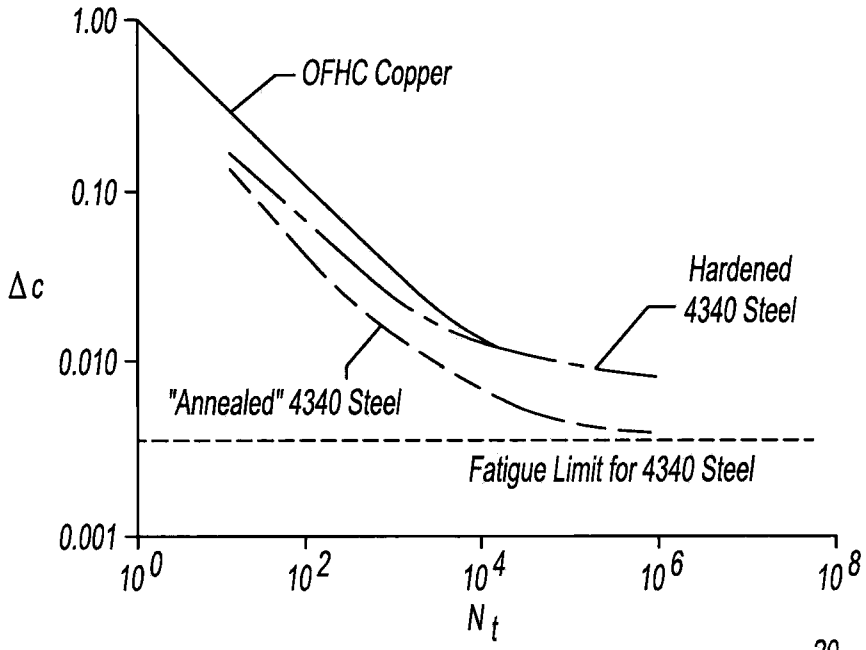


Fig-1

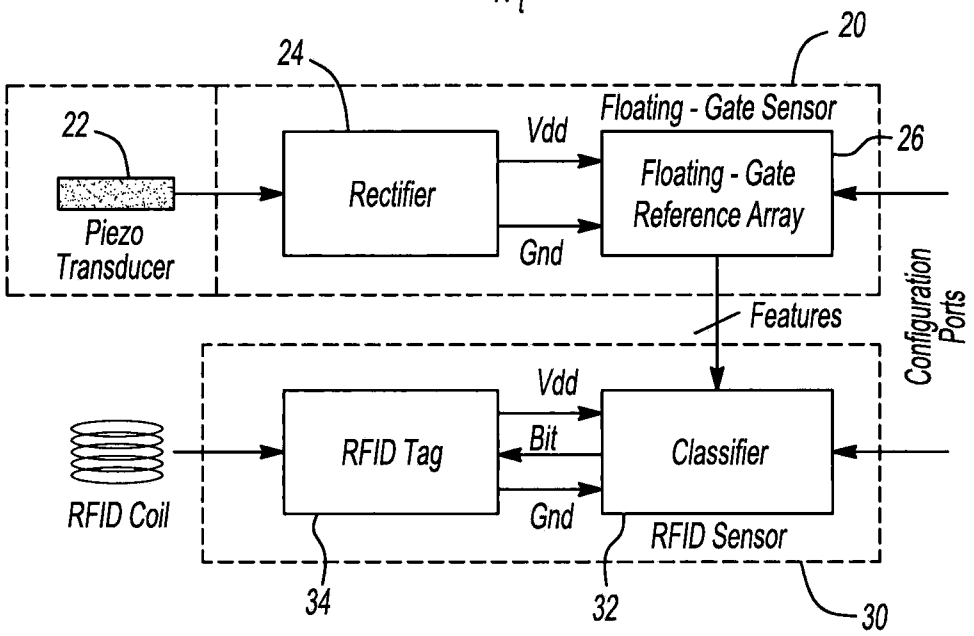


Fig-2

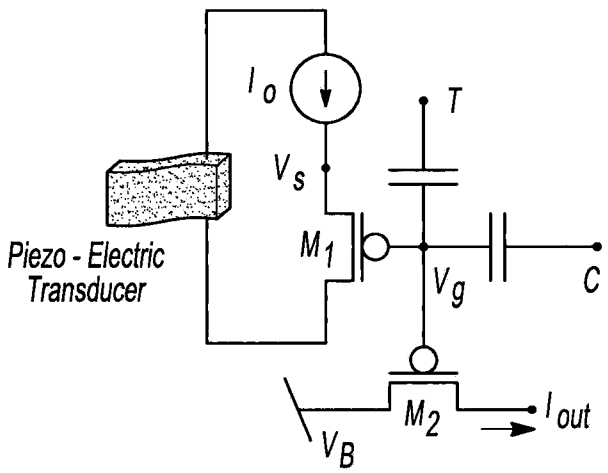


Fig-3

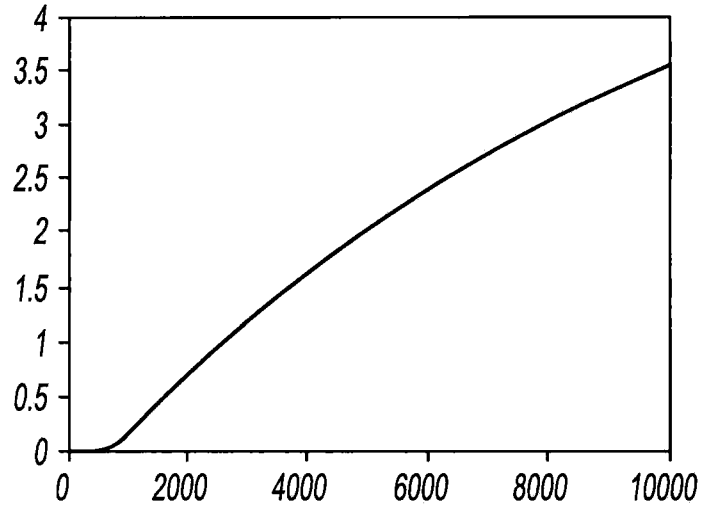

4
3.5
3
2.5
2
1.5
1
0.5
0
0
2000
4000
6000
8000
10000

Fig-4

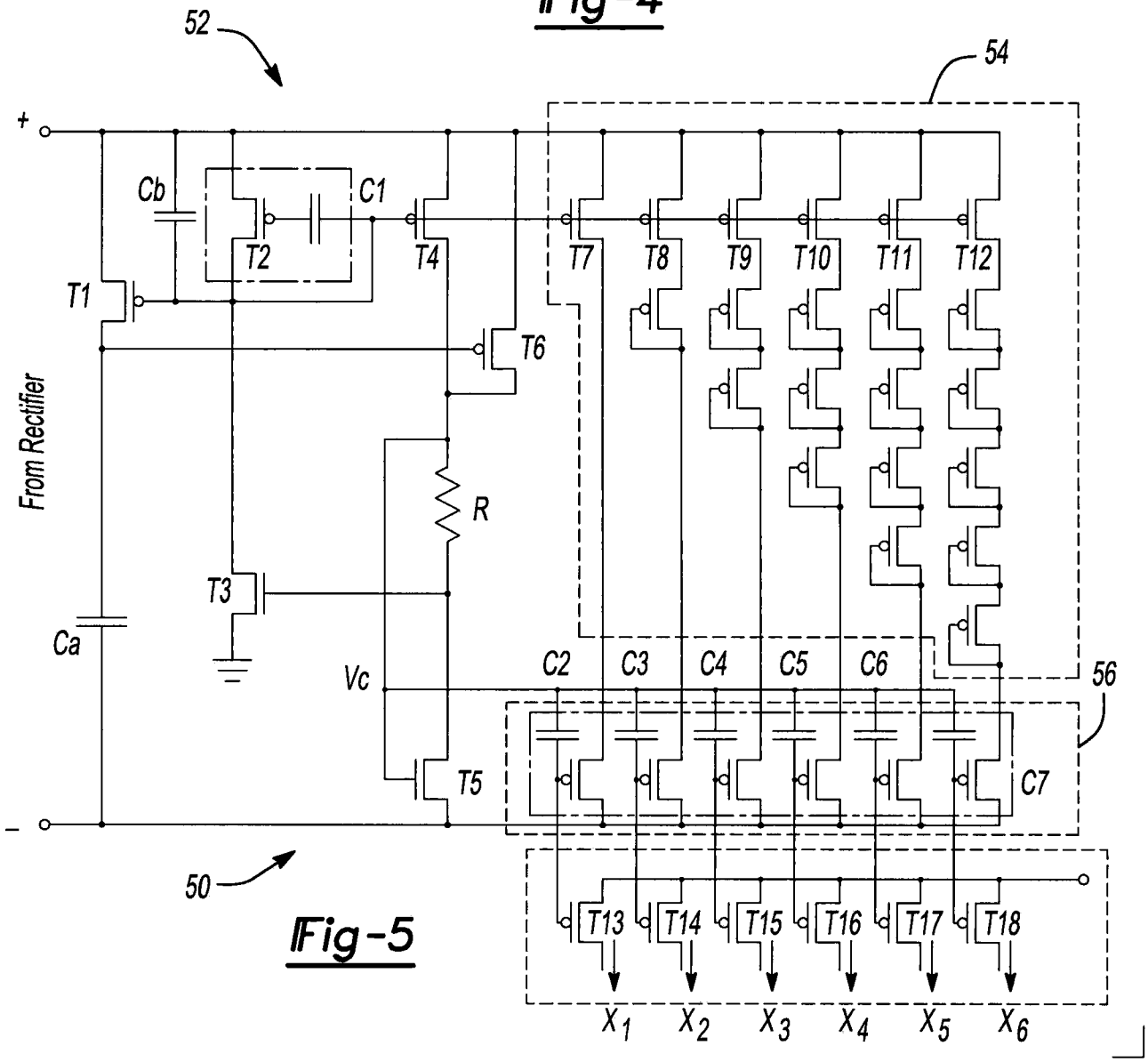

52
54
56
50
+
–
Cb
C1
T2
T4
T7
T8
T9
T10
T11
T12
T1
T6
From Rectifier
R
T3
Ca
Vc
C2
C3
C4
C5
C6
C7
T5
T13
T14
T15
T16
T17
T18
X1
X2
X3
X4
X5
X6

Fig-5

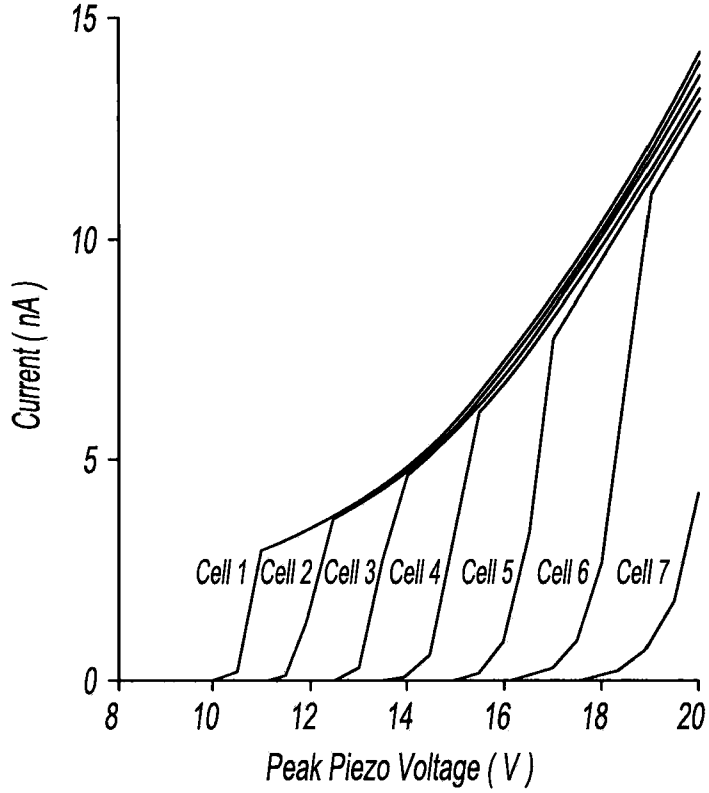

15
10
5
0
Current (nA)
Cell 1
Cell 2
Cell 3
Cell 4
Cell 5
Cell 6
Cell 7
8
10
12
14
16
18
20
Peak Piezo Voltage (V)

Fig-6

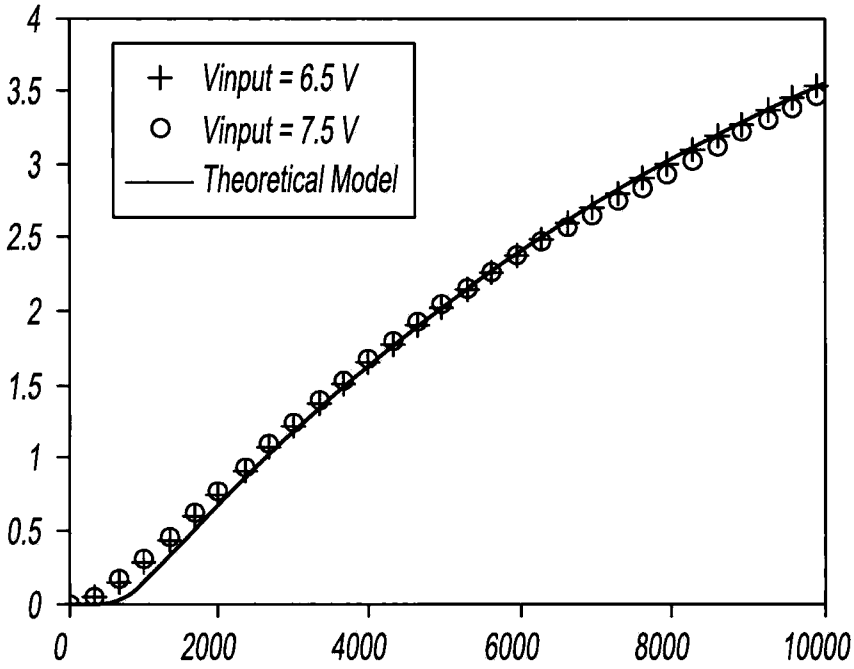

4
3.5
3
2.5
2
1.5
1
0.5
0
Vinput = 6.5 V
Vinput = 7.5 V
Theoretical Model
0
2000
4000
6000
8000
10000

Fig-7

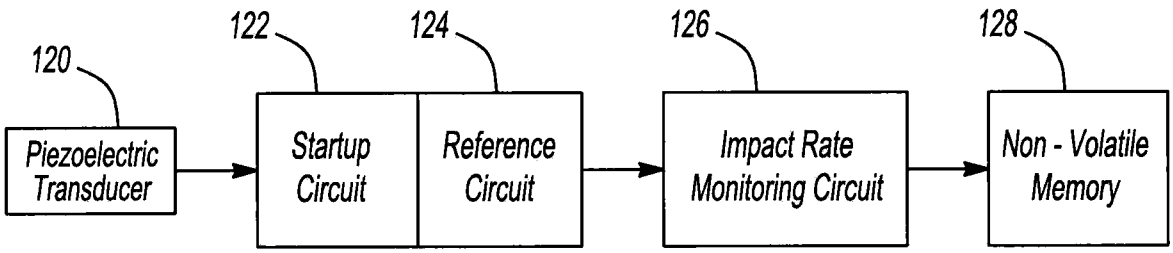


Fig-8

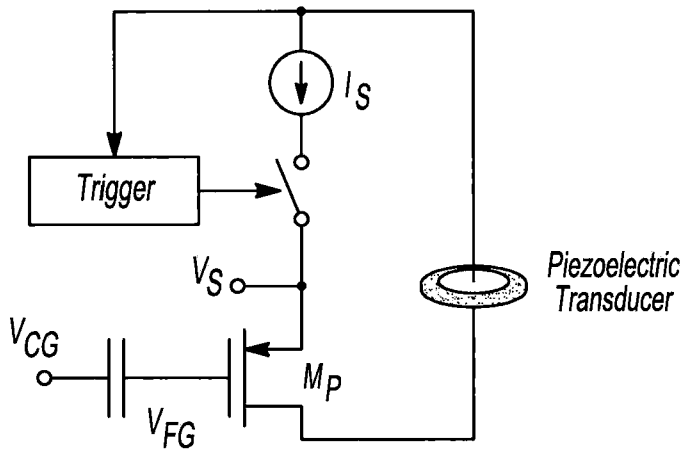


Fig-9

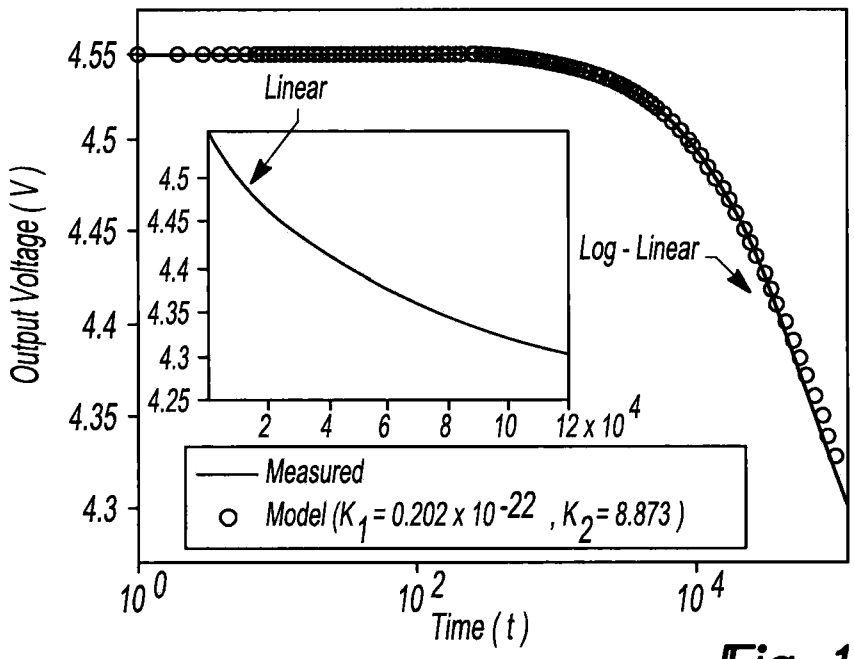


Fig-11

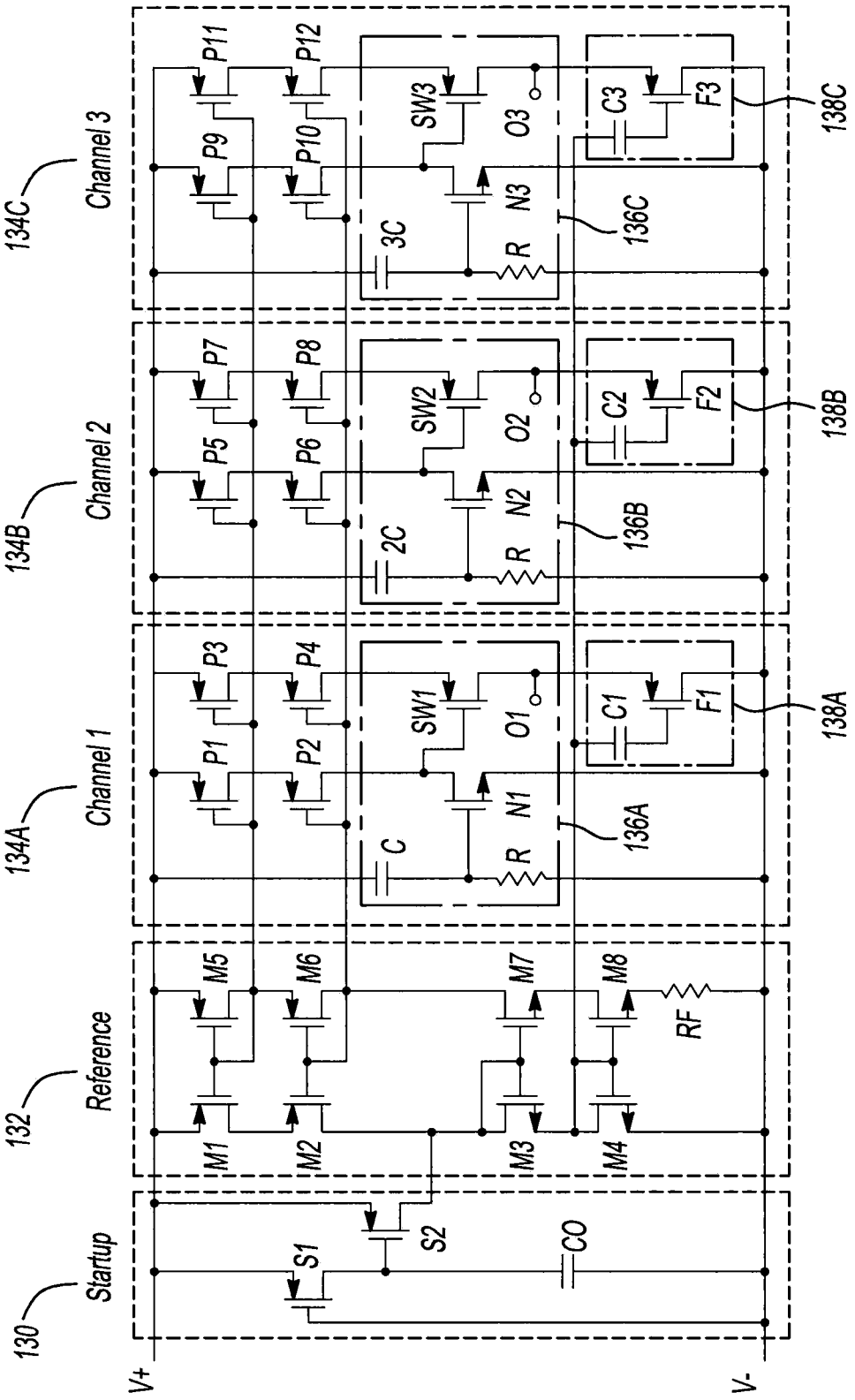

130
Startup
132
Reference
134A
Channel 1
134B
Channel 2
134C
Channel 3
V+
V-
S1
S2
CO
M1
M2
M3
M4
M5
M6
M7
M8
RF
P1
P2
P3
P4
P5
P6
P7
P8
P9
P10
P11
P12
C
2C
3C
R
N1
N2
N3
SW1
SW2
SW3
O1
O2
O3
136A
136B
136C
C1
C2
C3
F1
F2
F3
138A
138B
138C

Fig-10

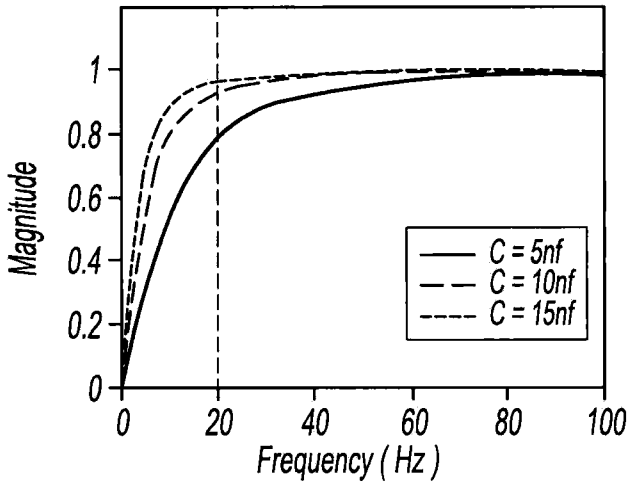


Fig-12

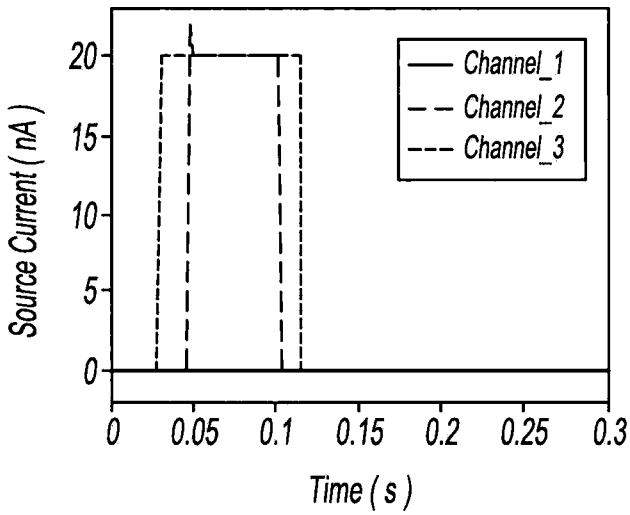


Fig-13

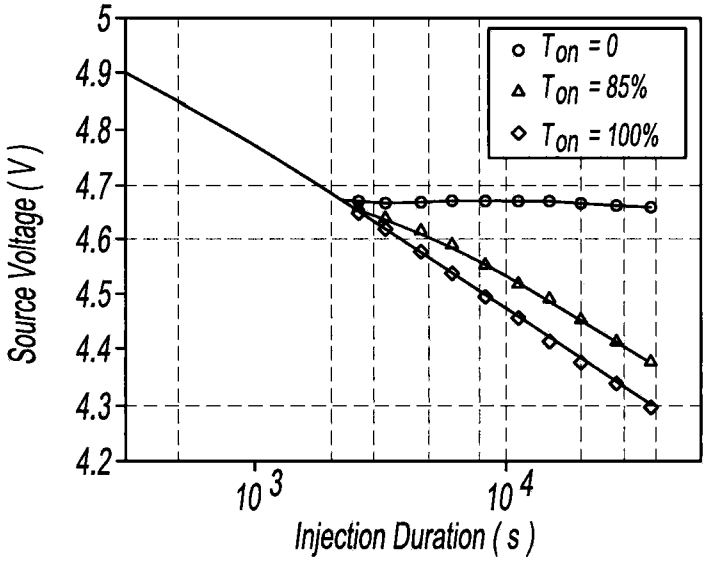


Fig-14

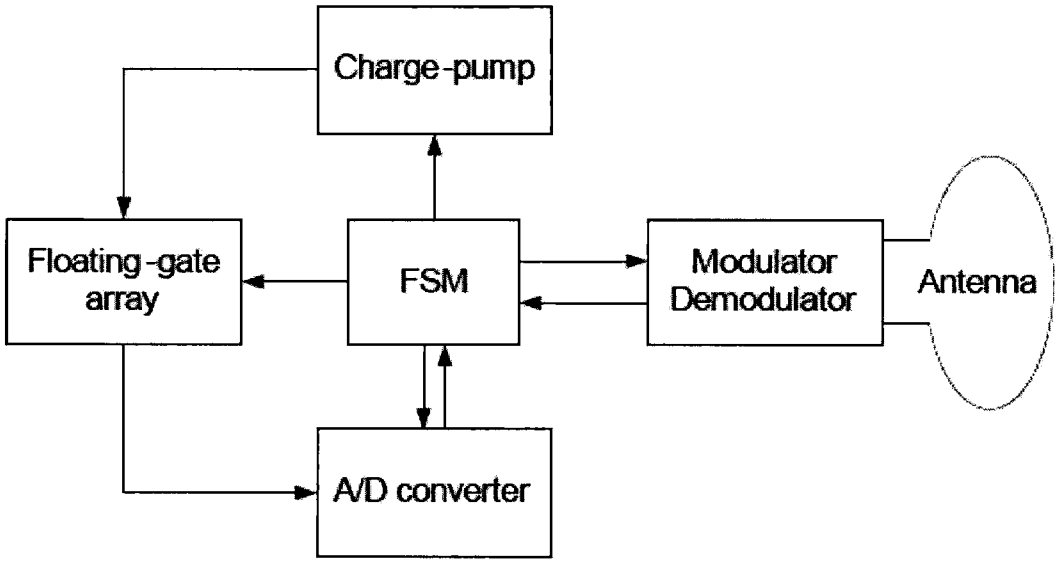

Charge-pump
Floating-gate array
FSM
Modulator Demodulator
Antenna
A/D converter

FIG. 15

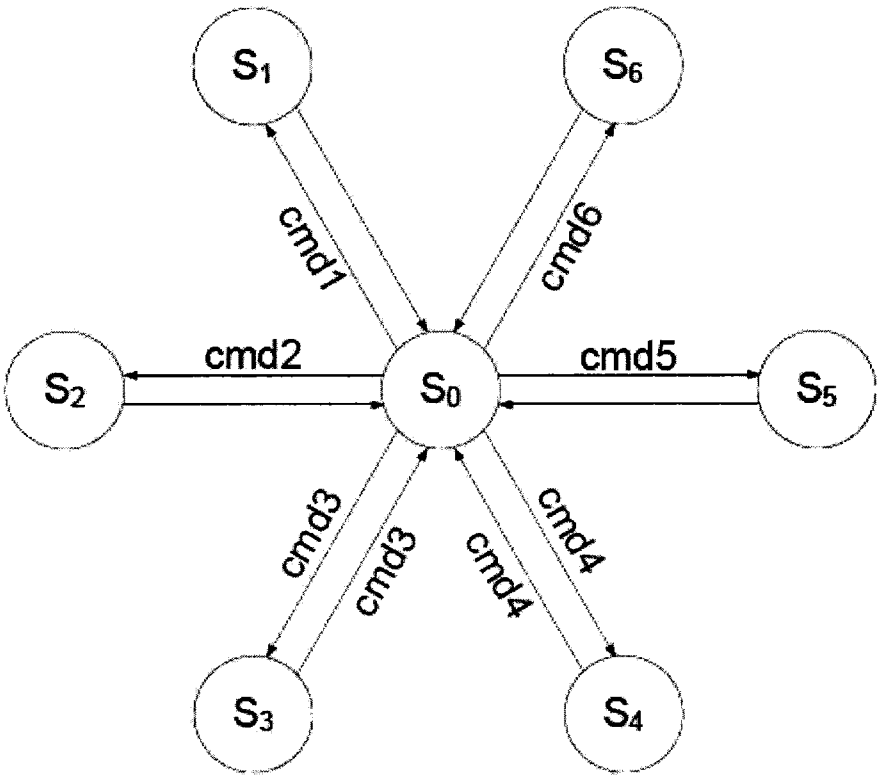


FIG. 16

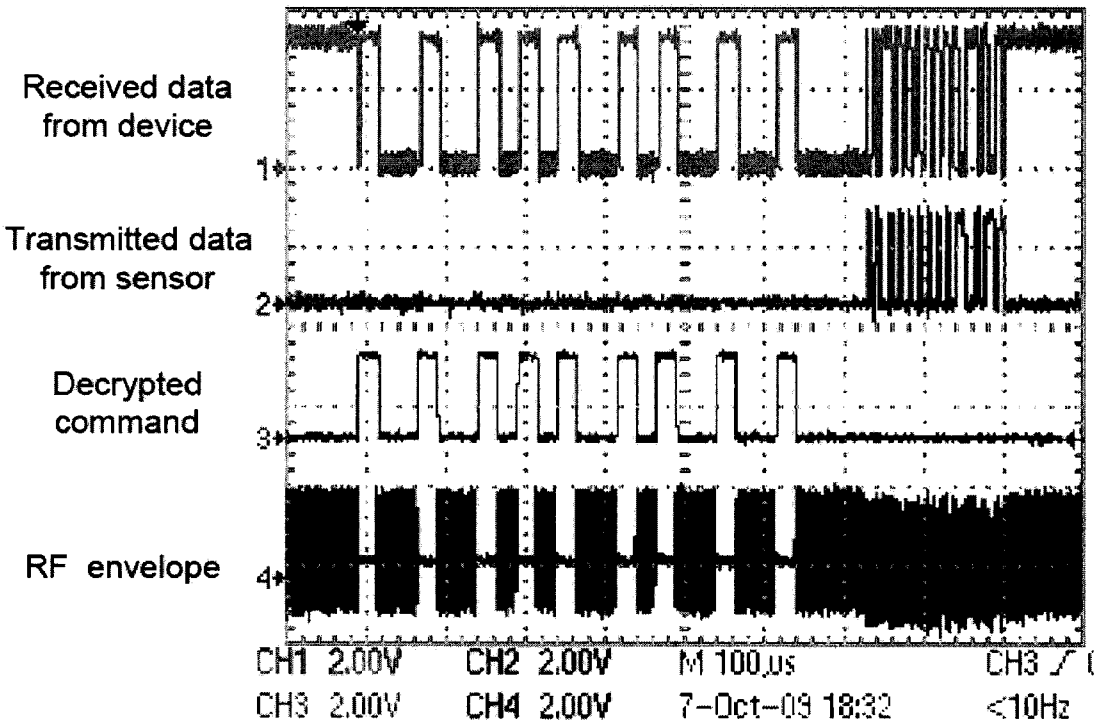

Received data from device
Transmitted data from sensor
Decrypted command
RF envelope
1
2
3
4
CH1 2.00V
CH2 2.00V
M 100µs
CH3
CH3 2.00V
CH4 2.00V
7-Oct-09 18:32
<10Hz

FIG. 17

INTERNATIONAL SEARCH REPORT

International application No
PCT/US2009/064019

A. CLASSIFICATION OF SUBJECT MATTER
INV. A61F2/46 G01M5/00

According to International Patent Classification (IPC) or to both national classification and IPC

B. FIELDS SEARCHED

Minimum documentation searched (classification system followed by classification symbols)
A61F G01M

Documentation searched other than minimum documentation to the extent that such documents are included in the fields searched

Electronic data base consulted during the international search (name of data base and, where practical, search terms used)
EPO-Internal, WPI Data

C. DOCUMENTS CONSIDERED TO BE RELEVANT

Category*	Citation of document, with indication, where appropriate, of the relevant passages	Relevant to claim No.
A	US 2008/047355 A1 (CHAKRABARTTY SHANTANU [US] ET AL) 28 February 2008 (2008-02-28) paragraphs [0019] - [0030]; figure 2	1,16,21, 26
A	EP 1 863 317 A2 (LOCKHEED CORP [US]) 5 December 2007 (2007-12-05) paragraphs [0038], [0039]; figure 1	1,16,21, 26

-/--

[X] Further documents are listed in the continuation of Box C.

[X] See patent family annex.

* Special categories of cited documents :

"A" document defining the general state of the art which is not considered to be of particular relevance

"E" earlier document but published on or after the international filing date

"L" document which may throw doubts on priority claim(s) or which is cited to establish the publication date of another citation or other special reason (as specified)

"O" document referring to an oral disclosure, use, exhibition or other means

"P" document published prior to the international filing date but later than the priority date claimed

"T" later document published after the international filing date or priority date and not in conflict with the application but cited to understand the principle or theory underlying the invention

"X" document of particular relevance; the claimed invention cannot be considered novel or cannot be considered to involve an inventive step when the document is taken alone

"Y" document of particular relevance; the claimed invention cannot be considered to involve an inventive step when the document is combined with one or more other such documents, such combination being obvious to a person skilled in the art.

"&" document member of the same patent family

Date of the actual completion of the international search	Date of mailing of the international search report
26 February 2010	10/03/2010

Name and mailing address of the ISA/	Authorized officer
European Patent Office, P.B. 5818 Patentlaan 2 NL - 2280 HV Rijswijk Tel. (+31-70) 340-2040, Fax: (+31-70) 340-3016	Steiner, Markus

INTERNATIONAL SEARCH REPORT

International application No
PCT/US2009/064019

C(Continuation). DOCUMENTS CONSIDERED TO BE RELEVANT

Category*	Citation of document, with indication, where appropriate, of the relevant passages	Relevant to claim No.
A	LAJNEF N ET AL: "A Piezo-Powered Floating-Gate Sensor Array for Long-Term Fatigue Monitoring in Biomechanical Implants" IEEE TRANSACTIONS ON BIOMEDICAL CIRCUITS AND SYSTEMS, IEEE, US, vol. 2, no. 3, 1 September 2008 (2008-09-01), pages 164-172, XP011237172 ISSN: 1932-4545 the whole document	1,16,21, 27
A	LAJNEF N ET AL: "Calibration and characterization of self-powered floating-gate sensor arrays for long-term fatigue monitoring" CIRCUITS AND SYSTEMS, 2008. ISCAS 2008. IEEE INTERNATIONAL SYMPOSIUM ON, IEEE, PISCATAWAY, NJ, USA, 18 May 2008 (2008-05-18), pages 1096-1099, XP031271649 ISBN: 978-1-4244-1683-7 paragraph 3 - page 1098, right-hand column, paragraph 1	1,16,21, 26

INTERNATIONAL SEARCH REPORT

Information on patent family members

International application No
PCT/US2009/064019

Patent document cited in search report	Publication date	Patent family member(s)	Publication date
US 2008047355 A1	28-02-2008	NONE	
EP 1863317 A2	05-12-2007	US 2007265790 A1	15-11-2007